HHS Public Access

Author manuscript

Mol Cancer Ther. Author manuscript; available in PMC 2017 August 01.

Published in final edited form as:

Mol Cancer Ther. 2016 August ; 15(8): 1859–1869. doi:10.1158/1535-7163.MCT-16-0025.

The combination of vemurafenib and procaspase-3 activation is synergistic in mutant BRAF melanomas

Jessie Peh[1,2], **Timothy M. Fan**[2,3], **Kathryn L. Wycislo**[4], **Howard S. Roth**[1,2], and **Paul J. Hergenrother**[1,2,*]

[1]Department of Chemistry, University of Illinois at Urbana-Champaign, Urbana, Illinois, USA.

[2]Institute for Genomic Biology, University of Illinois at Urbana-Champaign, Urbana, Illinois, USA.

[3]Department of Veterinary Clinical Medicine, University of Illinois at Urbana-Champaign, Urbana, Illinois, USA.

[4]Department of Pathobiology, University of Illinois at Urbana-Champaign, Urbana, Illinois, USA.

Abstract

The development of vemurafenib resistance limits the long-term efficacy of this drug for treatment of metastatic melanomas with the ^{V600E}BRAF mutation. Inhibition of downstream MAPK signaling with vemurafenib induces apoptotic cell death mediated by caspase-3, suggesting that addition of a procaspase-3 activator could enhance anticancer effects. Here we show that the combination of PAC-1, a procaspase-activating compound, and vemurafenib is highly synergistic in enhancing caspase-3 activity and apoptotic cell death in melanoma cell lines harboring the ^{V600E}BRAF mutation. *In vivo*, the combination displays a favorable safety profile in mice, and exerts significant antitumor effects. We further demonstrate that addition of PAC-1 to the clinically useful combination of vemurafenib and a MEK inhibitor, trametinib, starkly enhances the caspase-3 activity and proapoptotic effect of the combination. Moreover, addition of low concentration PAC-1 also delays the regrowth of cells following treatment with vemurafenib. Finally, PAC-1 remains potent against vemurafenib-resistant A375VR cells in cell culture and synergizes with vemurafenib to exert antitumor effects on A375VR cell growth *in vivo*. Collectively, our data suggest that inhibition of MAPK signaling combined with concurrent procaspase-3 activation is an effective strategy to enhance the antitumor activity of vemurafenib and mitigate the development of resistance.

Keywords

Cancer; Chemical biology; Medical research; Medicinal chemistry; Melanoma

Corresponding author: Paul J. Hergenrother, Department of Chemistry, University of Illinois, 261 Roger Adams Lab Box 36-5, 600 S. Mathews, Urbana, IL 61801, hergenro@uiuc.edu, phone # : (217) 333-0363, fax # : (217) 244-8024.

Conflict of interest:

The University of Illinois has filed patents on PAC-1, and these patents have been licensed by Vanquish Oncology. P. J. Hergenrother and T. M. Fan have ownership interest in Vanquish Oncology and have received funding from Vanquish Oncology.

Introduction

Melanoma is the most common cutaneous malignancy and upon metastasis is considered the deadliest form of skin cancer.(1) The discovery that approximately 50% of melanomas harbor the V600E mutation in the BRAF protein(2) spurred the development of ^{V600E}BRAF inhibitors,(3,4) and the subsequent approval of vemurafenib in 2011. ^{V600E}BRAF inhibitors like vemurafenib (and dabrafenib, approved in 2013) lead to impressive reduction in tumor burden within weeks of therapy, and extension of progression-free survival by three to four months.(5,6) Despite their initial anti-melanoma activity, resistance to ^{V600E}BRAF inhibitors rapidly emerges. In the majority of resistant tumors, reactivation of the MAPK signaling pathway is observed,(7) motivating the addition of MEK1/2 inhibitors (e.g. trametinib) to the treatment regimen for metastatic melanoma. Upfront combination therapy with MEK1/2 and ^{V600E}BRAF inhibitors is effective in delaying the median time to resistance by 3.7 to 4.1 months in patients who have not received prior ^{V600E}BRAF inhibition treatment,(8,9) but the addition of MEK1/2 inhibitor to patients who have already failed prior ^{V600E}BRAF inhibitor therapy only results in a marginal improvement in anticancer efficacy.(10) Given the current clinical limitations of existing therapies, novel and rationally-designed combination studies with other kinase inhibitors are being explored.(11,12) Despite all efforts to date, the development of resistance to targeted ^{V600E}BRAF therapies emerges in virtually 100% of patients treated; acquired drug resistance to this class of agents remains a significant obstacle to dramatically enhanced survival benefits for metastatic melanoma patients.

In contrast to many studies that have focused on the combination of vemurafenib with inhibitors of diverse and druggable kinases, combination therapy of vemurafenib with agents that activate the apoptotic pathway have not been extensively explored. In part, this lack of exploration might be attributed to the fact that melanoma cells possess multiple defects in their apoptotic signaling pathways,(13–15) rendering them resistant to many proapoptotic stimuli. We hypothesized that a suitable proapoptotic agent that induces apoptosis downstream of these apoptotic defects would be highly synergistic with ^{V600E}BRAF inhibitors.

Given that the aberrations in the apoptotic signaling cascades in melanoma cells are upstream of the activation of procaspase-3, drugs that directly activate procaspase-3 are intriguing candidates for this combination therapy. In addition, because melanomas have elevated expression of procaspase-3,(16,17) a procaspase-3 activator should be potent and selective for such cells. Furthermore, it is known that ^{V600E}BRAF inhibitors induce apoptotic cell death mediated by caspase-3;(3) thus, the combination of vemurafenib with a direct procaspase-3 activator could lead to dramatically enhanced caspase-3 activity and cancer cell death relative to the effect of either single-agent. PAC-1 (Fig. 1A) is a small molecule that directly activates cellular procaspase-3 via chelation of labile inhibitory zinc.(18–22) Due to the overexpression of procaspase-3 in cancers of diverse origins,(16,17,23–32) PAC-1 and its derivatives selectively induce apoptosis in cancer cells while sparing non-cancerous cells.(21,25,33,34) PAC-1 exerts single agent activity in multiple murine models of cancer,(21,34–36) including a xenograft model of melanoma.(21) Importantly, in addition to favorable preclinical activity in murine tumor models, human cancer patients have been taking PAC-1 as part of a Phase I clinical trial since March 2015 (NCT02355535).

Here we report the synergistic activity of PAC-1+vemurafenib and PAC-1+vemurafenib +trametinib in enhancement of caspase-3 activity and apoptotic cell death in ^{V600E}BRAF melanoma. As a result of increased apoptotic cell death, the PAC-1+vemurafenib combination induces significant reduction in tumor volume in a murine xenograft model of ^{V600E}BRAF melanoma, beyond the antitumor effects of the individual agents. In addition, this enhancement of apoptotic death in vemurafenib-sensitive melanoma by the addition of PAC-1 significantly delays the regrowth of cells after exposure to vemurafenib. Finally, PAC-1 remains effective in vemurafenib-resistant A375VR cells in culture and synergizes with vemurafenib to retard tumor growth of these cells *in vivo*, suggesting utility of this combination in melanomas that have progressed beyond BRAF-inhibitor treatment, for which few options for treatment are currently available.

Materials and Methods

Cell culture and reagents

A375 (CRL-1619) and CHL-1 (CRL-9446) were purchased from ATCC on 11/5/2014 and 11/18/2014 respectively. A375SM was provided by Prof. Isiah Fidler (MD Anderson, Texas) on 10/30/2014. All cell lines except B16-F10, H460, and HCT 116 were cultured in DMEM supplemented with 10% FBS (Gemini). B16-F10, H460, and HCT 116 were cultured in RPMI with 10% FBS. Vemurafenib, trametinib and Annexin V-FITC (10040-02) were purchased from LC Laboratories, MedChemExpress, and SouthernBiotech respectively. The following antibodies were purchased from Cell Signalling Technology: anti-PARP-1 (9542), anti-caspase-3 (9662), anti-β-actin (4967), anti-phospho-ERK1/2 (Thr202/Tyr204) (4370), anti-ERK1/2 (4695) and anti-rabbit IgG HRP linked (7074). Anti-cleaved-PARP-1 (ab32561) antibody was purchased from Epitomics. PAC-1 and PAC-1a were synthesized as previously reported.(34)

Cell line authentication

All human cell lines (A375, A375SM, CHL-1, H460, HCT 116, MIA PaCa-2, SK-MEL-5, and UACC-62) have been authenticated using the PowerPlex16HS Assay (Promega): 15 Autosomal Loci, X/Y at the University of Arizona Genetics Core. The results of the test (last performed: 9/18/2015) and pherograms can be found in the Supplementary Information. Mycoplasma testing has been performed for the A375 cell line using the Mycoplasma detect PCR at the University of Illinois Veterinary Diagnostic Lab on May 13, 2015. Results can also be found in the Supplementary Information.

Cellular proliferation assays

1000 – 2000 cells were seeded per well in a 96-well plate and allowed to adhere before DMSO solutions of PAC-1 or vemurafenib were added to each well. Proliferation was assessed by the sulforhodamine B (SRB) assay.

Annexin V/PI flow cytometry analysis

70,000 cells were seeded in 12-well plates and allowed to adhere before addition of compounds. Cells were treated with compounds for 24 h at 37 ^{o}C, after which they were harvested and resuspended in 450 μL of cold buffer (10 mM HEPES, 140 mM NaCl, 2.5

mM $CaCl_2$ pH 7.4) premixed with Annexin V-FITC and PI (0.55 μg/mL) dyes. Samples were analyzed on a BD Biosciences LSR II flow cytometer and data analysis was performed using FCS Express V3-2.

Caspase-3/7 activity assay

5,000–8,000 cells were plated in 96 well plates and allowed to adhere. Cells were treated with 1 μM of staurosporine for 24 h or with 13 μM of raptinal(37) for 3 h as positive control, DMSO as negative control and indicated concentrations of PAC-1 and vemurafenib for 0, 2, 4, 7, 10, 12, 16, 20 or 24 h. Plates were then assessed for caspase-3/7 activity via addition of bifunctional lysis and activity buffer (200 mM HEPES, 400 mM NaCl, 40 mM DTT, 0.4 mM EDTA, 1% Triton-X, pH 7.4) with 20 μM of Ac-DEVD-AFC (Cayman Chemicals) as the fluorogenic substrate (λ_{ex}=400 nm, λ_{em}=505 nm). Plates were pre-incubated at 37 °C at 30 min in the Synergy multi-mode reader (BioTek) then read for 30 min at 3 min intervals. The slopes for each well were calculated. Activity is expresses as normalized to minimal and maximal activity observed within the assay.

In vitro resistance assay

800 A375 or UACC-62 cells were plated in 96-well plates and allowed to attach overnight. The next day, vemurafenib (5 or 10 μM) or PAC-1 (1 μM) were treated in six technical replicates for 5, 10 and 20 days. Fresh media and compounds were added every 2–3 days for the duration of the study. At the end of 5, 10 or 20 days, the wells were fixed with 10% cold trichloroacetic acid for 1 h at 4 ºC. The wells were then washed, allowed to dry and stained with 0.5% SRB dye for 30 min at room temperature. The wells were then washed with 0.1% acetic acid and allowed to dry. At this point, images of the plates were taken with GelDoc XR (BioRad). Finally, 200 μL of 10 mM Tris base (pH > 10.4) was added into well and the absorbance at 510 nm were read using SpectraMax Plus (Molecular Devices). The absorbance at 510 nm is plotted against the days post treatment as an indication of cell proliferation over the time course of the experiment.

Immunoblotting

Cells and tumor tissues were lysed using RIPA buffer containing phosphatase and protease inhibitor cocktail (Calbiochem). The protein concentration of each sample was determined by the BCA assay (Pierce). Cell lysates containing 20 μg of protein was loaded into each lane of 4–20% gradient gels (BioRad) for SDS-PAGE. Proteins were transferred onto PDVF membrane for Western blot analysis.

PCR and sequencing

A375 and A375VR cells were lysed and RNA extracted using the RNeasy kit (Qiagen). 900 ng of RNA was used for reverse transcription reaction using iScript cDNA synthesis kit (BioRad). qPCR reactions were ran on the 7900HT fast real-time PCR system (Applied Biosystems). Regular PCR reactions were ran using the MyFi Mix PCR kit (Bioline) for 35 cycles and ran on a 1% agarose gel. Target amplicons were gel extracted and sequenced at the UIUC core sequencing facility. Primers used can be found in the Supplementary Information.

A375 and A375VR xenograft model

All animal studies were performed in accordance with UIUC IACUC guidelines (protocol no. 14292). 0.1 mL of A375 or A375VR in 1:1 DMEM:matrigel (Corning) was injected into the right flank of 6–7 (A375) or 5 (A375VR) week old female athymic nude mice (Charles River). In the both models, the mice were randomized into four groups: control, 100 mg/kg PAC-1, 10 mg/kg vemurafenib, and the combination of 100 mg/kg PAC-1 and 10 mg/kg vemurafenib (n=8). Initial tumor volume measurements were taken and dosing was initiated for a period of 15 days. Vemurafenib was formulated as 5% DMSO in 1% methyl cellulose and given twice daily by oral gavage (p.o.). PAC-1 was formulated in 200 mg/mL hydroxypropyl-β-cyclodextrin at pH 5.5 and given by intraperitoneal (i.p.) injection. Tumor length and width measurements were taken three times a week and volume was calculated as $0.52*L*W^2$. At the end of the study, the mice were euthanized and tumors were excised. The tumors were weighed and used for Western blot and immunohistochemistry.

Immunohistochemistry of A375 tumors and quantification of Ki-67 index

Immunohistochemistry (IHC) was performed on 4 μm-thick formalin-fixed paraffin-embedded A375 tumors after H&E staining confirmed the presence of a neoplastic cell population along with adequate tissue integrity. Antibody against Ki-67 (Biocare Medical #CRM325) was used for IHC and staining was visualized using the IntelliPATH FLX DAB chromogen kit (Biocare Medical #IPK 5010 G80). Human tonsil was used as the positive control tissue. Polymer negative control serum (mouse and rabbit) (Biocare Medical #NC499) was substituted for the primary antibody as a negative control. For quantification of Ki-67 index, 2000 neoplastic cells were counted and the percentage of positive cells was calculated. In tumors too small to quantify 2000 cells, the maximal number of neoplastic cells were counted. All slides were reviewed by a single veterinary pathologist (K.L.W.).

Results

The combination of PAC-1 and vemurafenib enhances apoptosis in cells with the ^{V600E}BRAF mutation

In a panel of nine cell lines of diverse origins and BRAF mutational status, vemurafenib is potent (IC_{50} values between 200 – 550 nM) only in cell lines harboring the ^{V600E}BRAF mutation, consistent with previously reported values (Fig. 1B).(3) Evaluation of PAC-1 in the same panel of cell lines shows that PAC-1 retains similar activity in all cell lines (IC_{50} values between 1–4 μM), regardless of BRAF mutational status (Fig. 1B). The ability of the combination of PAC-1+vemurafenib to induce apoptotic cell death was then assessed in these cell lines. Under conditions (24 h incubation with compounds) where neither vemurafenib nor PAC-1 induced significant apoptotic death (≤10%) as single agents, the PAC-1+vemurafenib combination induces significant apoptosis (20–45%) in cell lines with the ^{V600E}BRAF mutation (Fig. 1C). A similar trend was also observed when a lower concentration of vemurafenib (0.5 μM) was evaluated in combination with PAC-1 in ^{V600E}BRAF cell lines (Supplementary Fig. S1). However, the PAC-1+vemurafenib combination does not induce synergistic apoptosis in cell lines with wild-type BRAF (Fig. 1C).

PAC-1 and vemurafenib synergize to enhance caspase-3 activity and apoptosis in A375, SK-MEL-5 and UACC-62 cells

In order to more broadly explore the observed synergy, apoptotic death was assessed in three human ^{V600E}BRAF melanoma cell lines treated with a matrix of concentrations of PAC-1 and vemurafenib that induce minimal apoptosis as single agents. In these experiments, large increases in the populations of apoptotic cells (beyond the additive effect of single agents alone) were observed in A375 (Fig. 2A), SK-MEL-5 (Supplementary Fig. S2A) and UACC-62 (Supplementary Fig. S3A). To quantify the synergy of this drug combination, combination indices (CI) were calculated. A drug combination that is synergistic will have a CI value less than 1, while a value of 1 reflects an additive effect.(38) 93% of the calculated CI values are less than 1 (A375 in Fig. 2B, SK-MEL-5 in Supplementary Fig. S2B and UACC-62 in Supplementary Fig. S3B), indicating synergism for the combination across all three cell lines tested.

To assess if the increase in apoptosis was a result of increased activation of executioner procaspases, caspase-3/-7 enzymatic activity was evaluated in A375 cells (after lysis) using a fluorogenic substrate. In A375 cells treated with vemurafenib or PAC-1 alone (at the same concentrations used in Fig. 1C), negligible increases in caspase-3 activity were observed at these time points and concentrations (Fig. 2C). However, when A375 cells were treated with PAC-1 and vemurafenib, a significant increase in caspase-3 activity was observed as early as 7 h post-treatment (Fig. 2C). In Western blot analyses, neither of the single agents had an effect on PARP-1 cleavage at these time points and concentrations; however, the combination resulted in significant cleaved PARP-1 (Fig. 2D), a result of the increased caspase-3/-7 activity in cells treated with the PAC-1+vemurafenib combination. After treatment with the combination for 24 h, near-complete cleavage of PARP-1 was observed in A375 cells (Fig. 2D). Similar results for the caspase-3/-7 activity assay and cleavage of PARP-1 were also observed in SK-MEL-5 (Supplementary Fig. S2C and D) and UACC-62 cells (Supplementary Fig. S3C and D).

The PAC-1 derivative PAC-1a (Fig. 1A) lacks the zinc chelating motif and thus does not activate procaspase-3 or induce apoptosis.(18,34) Use of PAC-1a in combination with vemurafenib did not result in a significant increase in the proportion of cells undergoing apoptosis in A375, SK-MEL-5 or UACC-62 cells (Supplementary Fig. S4A-C). This result is also consistent with the absence of increased PARP-1 cleavage in cells treated with the PAC-1a and vemurafenib combination (Supplementary Fig. S4D), indicating that the cells did not undergo apoptotic death.

Inhibition of ERK1/2 phosphorylation and activation of procaspase-3 are required to enhance apoptotic cell death

Consistent with the data in Fig. 1C, no enhancement in caspase-3 activity or PARP-1 cleavage were observed in two ^{WT}BRAF cell lines when treated with the combination of PAC-1+vemurafenib (Supplementary Fig. S5A-C). The lack of PAC-1+vemurafenib synergy in cell lines harboring ^{WT}BRAF suggests that inhibition of ERK1/2 and activation of procaspase-3 are both required to induce the dramatic enhancement of apoptotic cell death. Indeed, after 24 h of treatment with vemurafenib, inhibition of ERK1/2 phosphorylation was

not observed in ^{WT}BRAF cell lines even at high concentrations (30 μM) of vemurafenib (Supplementary Fig. S5B and C). This observation is consistent with previous reports where vemurafenib does not inhibit ERK1/2 phosphorylation in ^{WT}BRAF cells, but paradoxically activates it.(3) To further investigate this, A375 (harboring ^{V600E}BRAF) cells were treated with PAC-1, vemurafenib, or the combination and probed for the presence of cleaved PARP-1 and ERK1/2 phosphorylation. After 24 h, phospho-ERK1/2 bands were not observed in cells treated with vemurafenib (at 0.5 and 1.0 μM) and the combination (Fig. 2E). However, significant increases in the amount of cleaved PARP-1 were only observed in cells treated with both PAC-1 and vemurafenib (Fig. 2E). Similar results were also observed in SK-MEL-5 (Supplementary Fig. S2E) and UACC-62 cells (Supplementary Fig. S3E). At low concentrations of vemurafenib (0.1 and 0.25 μM), where incomplete inhibition of ERK1/2 phosphorylation was observed, slight increase in PARP-1 cleavage over that single agent effects was also observed (Fig. 2E). This result suggests that even with incomplete inhibition of ERK1/2 phosphorylation, procaspase-3 activation, which is downstream of ERK1/2 signaling, can be enhanced with the addition of PAC-1 to vemurafenib treatments. Taken together, the data show that procaspase-3 activation via PAC-1 dramatically enhances the proapoptotic effect of vemurafenib in cell lines with ^{V600E}BRAF mutation.

Addition of PAC-1 to vemurafenib and trametinib enhances caspase-3 activity and apoptosis

Addition of a MEK1/2 inhibitor, such as trametinib, is widely used in the clinic to enhance the efficacy of vemurafenib in ^{V600E}BRAF melanomas.(8,9) To explore the effect of PAC-1 with this combination, cells were treated with vemurafenib+trametinib, in the presence or absence of PAC-1, and apoptosis was assessed. In both A375 and UACC-62 cell lines, vemurafenib+trametinib co-treatment led to mere additive increases in the population of apoptotic cells (Fig. 3A). In contrast, the addition of PAC-1 led to a large increase in the population of apoptotic cells, beyond the additive effect of single agents alone (Fig. 3A). Vemurafenib+trametinib co-treatment did not lead to PARP-1 cleavage, while addition of PAC-1 led to near quantitative cleavage of PARP-1 (Fig. 3B). To explore if the increased apoptotic cell death in the presence of PAC-1 is a result of enhanced enzymatic activity of executioner caspases, the caspase-3/-7 activity of A375 and UACC-62 cells treated with vemurafenib+trametinib, plus or minus PAC-1, was assessed. Again, a dramatic increase in caspase-3/-7 activity was observed when PAC-1 was included, an effect that was absent without addition of PAC-1 (Fig. 3C).

The combination of vemurafenib and PAC-1 significantly reduces tumor burden in an A375 xenograft model

To determine the antitumor effect of the PAC-1+vemurafenib combination *in vivo*, an A375 xenograft model(39) was used. In this model, nude mice were inoculated subcutaneously with A375 cells, and after allowing the tumors to grow, mice were randomized based upon tumor volume into four groups [$F=0.03 < F_{critical}(3.01)$] and dosed with PAC-1, vemurafenib, or the combination for 15 days. Treatment with PAC-1 alone led to minimal reduction in tumor mass and volume compared to untreated control mice (Fig. 4A and B). Mice dosed with vemurafenib alone experienced a moderate reduction (53%; $p=0.04$) in tumor volume and mass compared to control (Fig. 4A and B), with 3 out of 8 mice having

comparable tumor mass as the control mice (Fig. 4B). In contrast, mice treated with the combination of PAC-1 and vemurafenib had significantly smaller tumor burden compared to control mice (Fig. 4A, B and Supplementary Fig. S6). In these mice, a 78% reduction in tumor volume was observed (Fig. 4A, p=0.0008 vs. control), with 6 out of 8 mice having tumors less than 0.2 g in mass (Fig. 4B), suggesting that addition of PAC-1 enhances the antitumor effects of vemurafenib *in vivo* and reduces the variability in response to treatment.

Examination of procaspase-3 levels in the tumor samples by Western blot showed an appreciable and consistent reduction in the amount of procaspase-3 only in tumor samples derived from mice that received the combination treatment, versus variable responses for the other dosing groups (Fig. 4C and D). Using immunohistochemical staining, a significant reduction in the percentage of Ki-67 expressing cells in tumors treated with PAC-1+vemurafenib was observed (Fig. 4E), indicating that the PAC-1+vemurafenib combination was capable of not only amplifying procaspase-3 activation, but also attenuating cell proliferation. Finally, in mice treated with PAC-1+vemurafenib, no hematological toxicities were observed (Supplementary Table 1), indicating a favorable safety profile for the combination. Taken together, the *in vivo* data are consistent with the cell culture results showing that the synergy of PAC-1+vemurafenib leads to increase in caspase-3 activity and induction of apoptotic cell death, as well as reduction in cell proliferation.

Long term treatment with PAC-1 prevents cell regrowth, and addition of PAC-1 to vemurafenib delays the onset of cell regrowth

The E_{max} of vemurafenib (the percent cell death induced by high concentrations of compound)(40) in A375 cells is 96.8±0.3% after 5 days (Fig. 5A), indicating that ~3% of A375 cells are insensitive to vemurafenib. Under the same conditions, PAC-1 has an E_{max} of 99.4±0.7% (Fig. 5A), suggesting that PAC-1 kills A375 cells quantitatively, with very few insensitive cells. We therefore hypothesized that long term treatment with vemurafenib would lead to re-growth of cancer cells, while treatment with PAC-1 should prevent re-growth. To investigate this hypothesis, A375 and SK-MEL-5 cells were plated at low densities and treated continuously with PAC-1 (4 μM) or vemurafenib (10 μM) for up to 30 days. In A375 and SK-MEL-5 cells treated with vemurafenib, regrowth of cells was observed in as early as 20 days (Fig. 5B). However, in wells treated with PAC-1, no regrowth was observed even after 30 days (Fig. 5B). Thus, consistent with the higher E_{max} value, PAC-1 is able to quantitatively kill cells thereby preventing regrowth.

To investigate if addition of low concentrations of PAC-1 could combine with vemurafenib to prevent cancer cell re-growth, A375 and UACC-62 cells were plated at low densities in 96-well plates and treated continuously with PAC-1 (1 μM), vemurafenib (5 μM or 10 μM), or the combination for up to 20 days. After 5 days, treatment with PAC-1, vemurafenib, or the combination each resulted in significant reduction in cell number compared to the control (A375: Fig. 5C and D; UACC-62: Supplementary Fig. S7A and B). On day 10, there is no observable difference between the PAC-1 treated wells and the control. In wells treated with 5 μM or 10 μM vemurafenib, cell death was 89.4±1.4% and 93.2±1.1%, respectively. However, in wells where A375 cells were treated with 1 μM PAC-1 and 5 μM or 10 μM

vemurafenib, increased cell death was observed, 96.1±1.0% and 97.9±0.7% respectively. Consequent to achieving more complete cell death, a smaller proportion of cells remain in wells treated with both PAC-1 and vemurafenib. After 20 days of treatment, significant regrowth of colonies was observed in vemurafenib-only treated wells but not in wells receiving the co-treatment (A375: Fig. 5C and D; UACC-62: Supplementary Fig. S7A and B). This result indicates that the more complete cell death induced by co-treating cells with PAC-1 and vemurafenib is effective in delaying the regrowth of A375 and UACC-62.

PAC-1 synergizes with vemurafenib in vemurafenib-resistant melanoma in vivo

To assess if PAC-1 remains active in a cell line that has acquired resistance to vemurafenib, a vemurafenib-resistant A375VR cell line was generated by growing A375 parental cell line in sequentially higher concentrations of vemurafenib (0.5 μM to 1.0 μM) for 2 months. To determine the mechanism of resistance of A375VR, genes for MEK1/2, NRAS and AKT were sequenced, but no commonly reported mutations that would confer resistance were found.(41) Similarly, splice variant of the ^{V600E}BRAF mRNA was also not observed.(42) Through qPCR, A375VR cells have approximately 3-fold higher levels of MDR1 mRNA compared to A375. However, compared to up to 1000-fold higher levels of MDR1 mRNA in ovarian cells resistant to doxorubicin or cisplatin,(43) the level of MDR1 mRNA overexpression is considered low, indicating that resistance is unlikely due to dramatic upregulation of MDR phenotype.

Vemurafenib kills the A375VR cell line with a 5-day IC_{50} value of 1.5 μM, 12-fold less potent compared to the sensitivity of the parental A375 (Fig. 6A). Moreover, the vemurafenib E_{max} for A375VR is 79±6.3%, which is 14% lower than the parental A375 cell line. While treatment of parental A375 cells with vemurafenib (0.5 or 1 μM) for 2 h results in complete inhibition of ERK1/2 phosphorylation, this effect is not observed in A375VR, consistent with resistance of A375VR to vemurafenib and continued MAPK signaling (Fig. 6B). In contrast, PAC-1 retains activity against A375VR with an IC_{50} value of 2.4 μM (vs 1.2 μM for the parental cell line, Fig. 6C) and a similar E_{max}. We hypothesized that despite the inability of vemurafenib to inhibit ERK1/2 phosphorylation and MAPK signaling in the resistant A375VR cell line, the combination might retain partial capacity to exert a synergistic effect based on the PARP-1 cleavage observed for PAC-1+vemurafenib treatment, even under conditions of incomplete inhibition of ERK1/2 phosphorylation (Fig. 2E). To investigate if PAC-1 can re-sensitize A375VR cells to vemurafenib-induced apoptosis, A375VR cells were treated with PAC-1 in combination with low concentrations of vemurafenib. This combination treatment led to an increase in the proportion of cells undergoing apoptosis (Supplementary Fig. S8A, C), suggesting that the addition of PAC-1 can bypass the resistance mechanism of A375VR to vemurafenib. This effect was abolished when inactive variant PAC-1a was used (Supplementary Fig. S8C). The PAC-1+vemurafenib combination was synergistic, inducing an average of 7.5% higher population of apoptotic cells than predicted by the Bliss independence model(44) (Supplementary Fig. S8A and B). Finally, to determine if PAC-1 can synergize with vemurafenib *in vivo*, A375VR cells were implanted subcutaneously in nude mice, and the mice were dosed daily for 15 days with vemurafenib (10 mg/kg), PAC-1 (100 mg/kg) or the combination. Treatment with vemurafenib or PAC-1 alone does not exert any antitumor affect in this *in vivo* model, while

treatment with combination led to significant reduction in tumor volume compared to the untreated control (Fig. 6D).

Discussion

Given that the aberrations in the apoptotic signaling cascades in melanoma cells are upstream of the activation of procaspase-3, small molecules that directly activate procaspase-3 can induce apoptosis by bypassing the defective apoptotic circuitry. Activation of procaspase-3 with PAC-1 has been shown previously to have single agent efficacy against melanoma cells in culture,(21,33,34) and now we show that PAC-1+vemurafenib, or PAC-1+vemurafenib+trametinib, are powerfully synergistic in the induction of caspase-3 activity and apoptotic cell death in melanomas with ^{V600E}BRAF mutation. Besides melanomas, the ^{V600E}BRAF mutation has been reported in several other cancers including Erdheim-Chester disease (ECD) (54%)(45), Langerhans'-cell histiocytosis (LCH) (57%) (45), non-small-cell lung cancer (NSCLC) (1.5%)(46) and hairy-cell leukemia (100%)(47). In two recent Phase II trials, efficacy of vemurafenib in several non-melanoma cancers harboring the ^{V600E}BRAF mutation was reported, with promising results seen in patients with NSCLC, ECD, LCH and refractory hairy-cell leukemia.(48,49) Given this clinical data and our current work showing potent synergy between PAC-1, vemurafenib, and trametinib in ^{V600E}BRAF melanomas, these PAC-1/drug combinations could have efficacy in other malignancies harboring the ^{V600E}BRAF mutation.

The E_{max} parameter is a useful metric to assess the ability of a compound to quantitatively kill cancer cells in culture;(40) E_{max} values less than 100% imply heterogeneity in the ability of the drug to kill the cancer cell population. Here we show that vemurafenib has an E_{max} of ~97% in ^{V600E}BRAF mutant A375 cells, but the E_{max} value for PAC-1 approaches 100%. Because of this, no regrowth of A375 or SK-MEL-5 cells is observed in long-term experiments with PAC-1. However, extensive regrowth was observed in A375, UACC-62 and SK-MEL-5 cells treated only with vemurafenib for 20 days. With the addition of a low concentration of PAC-1 (1 μM) to vemurafenib, little to no regrowth was observed in cells. These results suggest that addition of low concentrations of PAC-1 (1 μM, a PAC-1 concentration that is readily achieved *in vivo*(50)) could be effective clinically in delaying resistance. The significant increase in caspase-3 activity, followed by massive induction of apoptosis early on during the combination treatment, likely kills off a large proportion of the cells that were initially insensitive to vemurafenib. Consequently, there is a significantly smaller residual population of cells that are unaffected by the treatment, crucial to delaying the regrowth of cells.

Currently, few options exist for patients who have developed vemurafenib-resistant melanomas. The MEK1/2 inhibitor, trametinib, though approved for melanomas with ^{V600E}BRAF mutation, exerts limited activity in combination with BRAF inhibitor in patients who have failed prior therapy.(10) Our results show that PAC-1 still synergizes with vemurafenib to exert antitumor effects in vemurafenib-resistant tumors. Therefore, addition of PAC-1 might be a viable and alternative therapeutic option for patients whose melanomas have progressed after vemurafenib treatment. The PAC-1+vemurafenib combination is well tolerated, has a good safety profile and exhibits significant antitumor effects *in vivo*. PAC-1

is currently in a Phase I clinical trial (NCT02355535), and both vemurafenib and trametinib are approved first-line treatment for ^{V600E}BRAF melanoma. There is thus a clear path to translate the preclinical demonstration of synergy described in this work to clinical trials where this novel combination can be assessed in human patients with cancers harboring the ^{V600E}BRAF mutation.

Supplementary Material

Refer to Web version on PubMed Central for supplementary material.

Acknowledgments

Financial support:

P. J. Hergenrother and T. M. Fan – National Institutes of Health Grant R01-CA120439 and University of Illinois

H. S. Roth – Richard B. Silverman Predoctoral Fellowship from the American Chemical Society Division of Medicinal Chemistry

References

1. Balch CM, Gershenwald JE, Soong S-j, Thompson JF, Atkins MB, Byrd DR, et al. Final version of 2009 AJCC melanoma staging and classification. J Clin Oncol. 2009; 27:6199–6206. [PubMed: 19917835]
2. Davies H, Bignell GR, Cox C, Stephens P, Edkins S, Clegg S, et al. Mutations of the BRAF gene in human cancer. Nature. 2002; 417:949–954. [PubMed: 12068308]
3. Joseph EW, Pratilas CA, Poulikakos PI, Tadi M, Wang W, Taylor BS, et al. The RAF inhibitor PLX4032 inhibits ERK signaling and tumor cell proliferation in a V600E BRAF-selective manner. Proc Natl Acad Sci U S A. 2010; 107:14903–14908. [PubMed: 20668238]
4. Rheault TR, Stellwagen JC, Adjabeng GM, Hornberger KR, Petrov KG, Waterson AG, et al. Discovery of dabrafenib: A selective inhibitor of Raf kinases with antitumor activity against B-Raf-driven tumors. ACS Med Chem Lett. 2013; 4:358–362. [PubMed: 24900673]
5. Chapman PB, Hauschild A, Robert C, Haanen JB, Ascierto P, Larkin J, et al. Improved survival with vemurafenib in melanoma with BRAF V600E mutation. N Engl J Med. 2011; 364:2507–2516. [PubMed: 21639808]
6. Hauschild A, Grob J-J, Demidov LV, Jouary T, Gutzmer R, Millward M, et al. Dabrafenib in BRAF-mutated metastatic melanoma: a multicentre, open-label, phase 3 randomised controlled trial. Lancet. 2012; 380:358–365. [PubMed: 22735384]
7. Holderfield M, Deuker MM, McCormick F, McMahon M. Targeting RAF kinases for cancer therapy: BRAF-mutated melanoma and beyond. Nat Rev Cancer. 2014; 14:455–467. [PubMed: 24957944]
8. Larkin J, Ascierto PA, Dréno B, Atkinson V, Liszkay G, Maio M, et al. Combined vemurafenib and cobimetinib in BRAF-mutated melanoma. N Engl J Med. 2014; 371:1867–1876. [PubMed: 25265494]
9. Robert C, Karaszewska B, Schachter J, Rutkowski P, Mackiewicz A, Stroiakovski D, et al. Improved overall survival in melanoma with combined dabrafenib and trametinib. N Engl J Med. 2014; 372:30–39. [PubMed: 25399551]
10. Kim KB, Kefford R, Pavlick AC, Infante JR, Ribas A, Sosman JA, et al. Phase II study of the MEK1/MEK2 Inhibitor trametinib in patients with metastatic BRAF-mutant cutaneous melanoma previously treated with or without a BRAF inhibitor. J Clin Oncol. 2013; 31:482–489. [PubMed: 23248257]
11. Atefi M, von Euw E, Attar N, Ng C, Chu C, Guo D, et al. Reversing melanoma cross-resistance to BRAF and MEK inhibitors by co-targeting the AKT/mTOR pathway. PLoS ONE. 2011; 6:e28973. [PubMed: 22194965]

12. Sweetlove M, Wrightson E, Kolekar S, Rewcastle GW, Baguley BC, Shepherd PR, et al. Inhibitors of pan PI3K signaling synergize with BRAF or MEK inhibitors to prevent BRAF-mutant melanoma cell growth. Front Oncol. 2015; 5
13. Soengas MS, Capodieci P, Polsky D, Mora J, Esteller M, Opitz-Araya X, et al. Inactivation of the apoptosis effector Apaf-1 in malignant melanoma. Nature. 2001; 409:207–211. [PubMed: 11196646]
14. Soengas MS, Lowe SW. Apoptosis and melanoma chemoresistance. Oncogene. 2003; 22:3138–3151. [PubMed: 12789290]
15. Hersey P, Zhang XD. How melanoma cells evade TRAIL-induced apoptosis. Nat Rev Cancer. 2001; 1:142–150. [PubMed: 11905805]
16. Chen N, Gong J, Chen X, Meng W, Huang Y, Zhao F, et al. Caspases and inhibitor of apoptosis proteins in cutaneous and mucosal melanoma: expression profile and clinicopathologic significance. Hum Pathol. 2009; 40:950–956. [PubMed: 19269012]
17. Fink D, Schlagbauer-Wadl H, Selzer E, Lucas T, Wolff K, Pehamberger H, et al. Elevated procaspase levels in human melanoma. Melanoma Res. 2001; 11:385–393. [PubMed: 11479427]
18. Peterson QP, Goode DR, West DC, Ramsey KN, Lee JJY, Hergenrother PJ. PAC-1 activates procaspase-3 in vitro through relief of zinc-mediated inhibition. J Mol Biol. 2009; 388:144–158. [PubMed: 19281821]
19. Peterson QP, Hsu DC, Goode DR, Novotny CJ, Totten RK, Hergenrother PJ. Procaspase-3 activation as an anti-cancer strategy: Structure-activity relationship of Procaspase-Activating Compound 1 (PAC-1) and its cellular co-localization with caspase-3. J Med Chem. 2009; 52:5721–5731. [PubMed: 19708658]
20. Putinski C, Abdul-Ghani M, Stiles R, Brunette S, Dick SA, Fernando P, et al. Intrinsic-mediated caspase activation is essential for cardiomyocyte hypertrophy. Proc Natl Acad Sci U S A. 2013; 110:E4079–E4087. [PubMed: 24101493]
21. Wang F, Wang L, Zhao Y, Li Y, Ping G, Xiao S, et al. A novel small-molecule activator of procaspase-3 induces apoptosis in cancer cells and reduces tumor growth in human breast, liver and gallbladder cancer xenografts. Mol Oncol. 2014; 8:1640–1652. [PubMed: 25053517]
22. Roth HS, Hergenrother PJ. Derivatives of Procaspase-Activating Compound 1 (PAC-1) and their Anticancer Activities. Curr Med Chem. 2016; 23:201–241. [PubMed: 26630918]
23. Soini Y, Paakko P. Apoptosis and expression of caspases 3, 6 and 8 in malignant non-Hodgkin's lymphomas. APMIS. 1999; 107:1043–1050. [PubMed: 10598877]
24. Estrov Z, Thall PF, Talpaz M, Estey EH, Kantarjian HM, Andreeff M, et al. Caspase 2 and caspase 3 protein levels as predictors of survival in acute myelogenous leukemia. Blood. 1998; 92:3090–3097. [PubMed: 9787143]
25. Patel V, Balakrishnan K, Keating MJ, Wierda WG, Gandhi V. Expression of executioner procaspases and their activation by a procaspase-activating compound in chronic lymphocytic leukemia cells. Blood. 2015; 125:1126–1136. [PubMed: 25538042]
26. Murphy AC, Weyhenmeyer B, Schmid J, Kilbride SM, Rehm M, Huber HJ, et al. Activation of executioner caspases is a predictor of progression-free survival in glioblastoma patients: a systems medicine approach. Cell Death Dis. 2013; 4:e629. [PubMed: 23681224]
27. Virkajarvi N, Paakko P, Soini Y. Apoptotic index and apoptosis influencing proteins bcl-2, mcl-1, bax and caspases 3, 6 and 8 in pancreatic carcinoma. Histopathology. 1998; 33:432–439. [PubMed: 9839167]
28. Krepela E, Prochazka J, Liu X, Fiala P, Kinkor Z. Increased expression of Apaf-1 and procaspase-3 and the functionality of intrinsic apoptosis apparatus in non-small cell lung carcinoma. Biol Chem. 2004; 385:153–168. [PubMed: 15101558]
29. O'Donovan N, Crown J, Stunell H, Hill ADK, McDermott E, O'Higgins N, et al. Caspase 3 in breast cancer. Clin Cancer Res. 2003; 9:738–742. [PubMed: 12576443]
30. Jiang H, Gong M, Cui Y, Ma K, Chang D, Wang TY. Upregulation of caspase-3 expression in esophageal cancer correlates with favorable prognosis: an immunohistochemical study from a high incidence area in northern China. Dis Esophagus. 2010; 23:487–492. [PubMed: 20113321]

31. Roy S, Bayly CI, Gareau Y, Houtzager VM, Kargman S, Keen SL, et al. Maintenance of caspase-3 proenzyme dormancy by an intrinsic "safety catch" regulatory tripeptide. Proc Natl Acad Sci USA. 2001; 98:6132–6137. [PubMed: 11353841]
32. Sadowska A, Car H, Pryczynicz A, Guzinska-Ustymowicz K, Kowal KW, Cepowicz D, et al. Expression of apoptotic proteins in human colorectal cancer and metastatic lymph nodes. Pathol Res Pract. 2014; 210:576–581. [PubMed: 24939147]
33. Peterson QP, Hsu DC, Novotny CJ, West DC, Kim D, Schmit JM, et al. Discovery and canine preclinical assessment of a nontoxic procaspase-3-activating compound. Cancer Res. 2010; 70:7232–7241. [PubMed: 20823163]
34. Putt KS, Chen GW, Pearson JM, Sandhorst JS, Hoagland MS, Kwon J-T, et al. Small-molecule activation of procaspase-3 to caspase-3 as a personalized anticancer strategy. Nat Chem Biol. 2006; 2:543–550. [PubMed: 16936720]
35. Razi SS, Rehmani S, Li X, Park K, Schwartz GS, Latif MJ, et al. Antitumor activity of paclitaxel is significantly enhanced by a novel proapoptotic agent in non-small cell lung cancer. J Surg Res. 2015; 194:622–630. [PubMed: 25498514]
36. Botham RC, Fan TM, Im I, Borst LB, Dirikolu L, Hergenrother PJ. Dual small-molecule targeting of procaspase-3 dramatically enhances zymogen activation and anticancer activity. J Am Chem Soc. 2014; 136:1312–1319. [PubMed: 24383395]
37. Palchaudhuri R, Lambrecht MJ, Botham RC, Partlow KC, van Ham TJ, Putt KS, et al. A Small Molecule that Induces Intrinsic Pathway Apoptosis with Unparalleled Speed. Cell Rep. 2015; 13:2027–2036. [PubMed: 26655912]
38. Chou T-C. Theoretical basis, experimental design, and computerized simulation of synergism and antagonism in drug combination studies. Pharmacol Rev. 2006; 58:621–681. [PubMed: 16968952]
39. Yadav V, Burke TF, Huber L, Van Horn RD, Zhang Y, Buchanan SG, et al. The CDK4/6 Inhibitor LY2835219 overcomes vemurafenib resistance resulting from MAPK reactivation and cyclin D1 upregulation. Mol Cancer Ther. 2014; 13:2253–2263. [PubMed: 25122067]
40. Fallahi-Sichani M, Honarnejad S, Heiser LM, Gray JW, Sorger PK. Metrics other than potency reveal systematic variation in responses to cancer drugs. Nat Chem Biol. 2013; 9:708–714. [PubMed: 24013279]
41. Rizos H, Menzies AM, Pupo GM, Carlino MS, Fung C, Hyman J, et al. BRAF Inhibitor Resistance Mechanisms in Metastatic Melanoma: Spectrum and Clinical Impact. Clinical Cancer Research. 2014; 20:1965–1977. [PubMed: 24463458]
42. Poulikakos PI, Persaud Y, Janakiraman M, Kong X, Ng C, Moriceau G, et al. RAF inhibitor resistance is mediated by dimerization of aberrantly spliced BRAF(V600E). Nature. 2011; 480:387–390. [PubMed: 22113612]
43. Januchowski R, Wojtowicz K, Sujka-Kordowska P, Andrzejewska M, Zabel M. MDR Gene Expression Analysis of Six Drug-Resistant Ovarian Cancer Cell Lines. BioMed Res Intl. 2013; 2013:10.
44. Bliss CI. The toxicity of poisons applied jointly. Ann Appl Biol. 1939; 26:585–615.
45. Haroche J, Charlotte F, Arnaud L, von Deimling A, Hélias-Rodzewicz Z, Hervier B, et al. High prevalence of BRAF V600E mutations in Erdheim-Chester disease but not in other non-Langerhans cell histiocytoses. Blood. 2012; 120:2700–2703. [PubMed: 22879539]
46. Cardarella S, Ogino A, Nishino M, Butaney M, Shen J, Lydon C, et al. Clinical, pathologic, and biologic features associated with BRAF mutations in non–small cell lung cancer. Clin Cancer Res. 2013; 19:4532–4540. [PubMed: 23833300]
47. Tiacci E, Trifonov V, Schiavoni G, Holmes A, Kern W, Martelli MP, et al. BRAF mutations in hairy-cell leukemia. N Engl J Med. 2011; 364:2305–2315. [PubMed: 21663470]
48. Hyman DM, Puzanov I, Subbiah V, Faris JE, Chau I, Blay J-Y, et al. Vemurafenib in Multiple Nonmelanoma Cancers with BRAF V600 Mutations. N Engl J Med. 2015; 373:726–736. [PubMed: 26287849]
49. Tiacci E, Park JH, De Carolis L, Chung SS, Broccoli A, Scott S, et al. Targeting Mutant BRAF in Relapsed or Refractory Hairy-Cell Leukemia. N Engl J Med. 2015; 373:1733–1747. [PubMed: 26352686]

50. Lucas PW, Schmit JM, Peterson QP, West DC, Hsu DC, Novotny CJ, et al. Pharmacokinetics and derivation of an anticancer dosing regimen for PAC-1, a preferential small molecule activator of procaspase-3, in healthy dogs. Invest New Drugs. 2011; 29:901–911. [PubMed: 20499133]

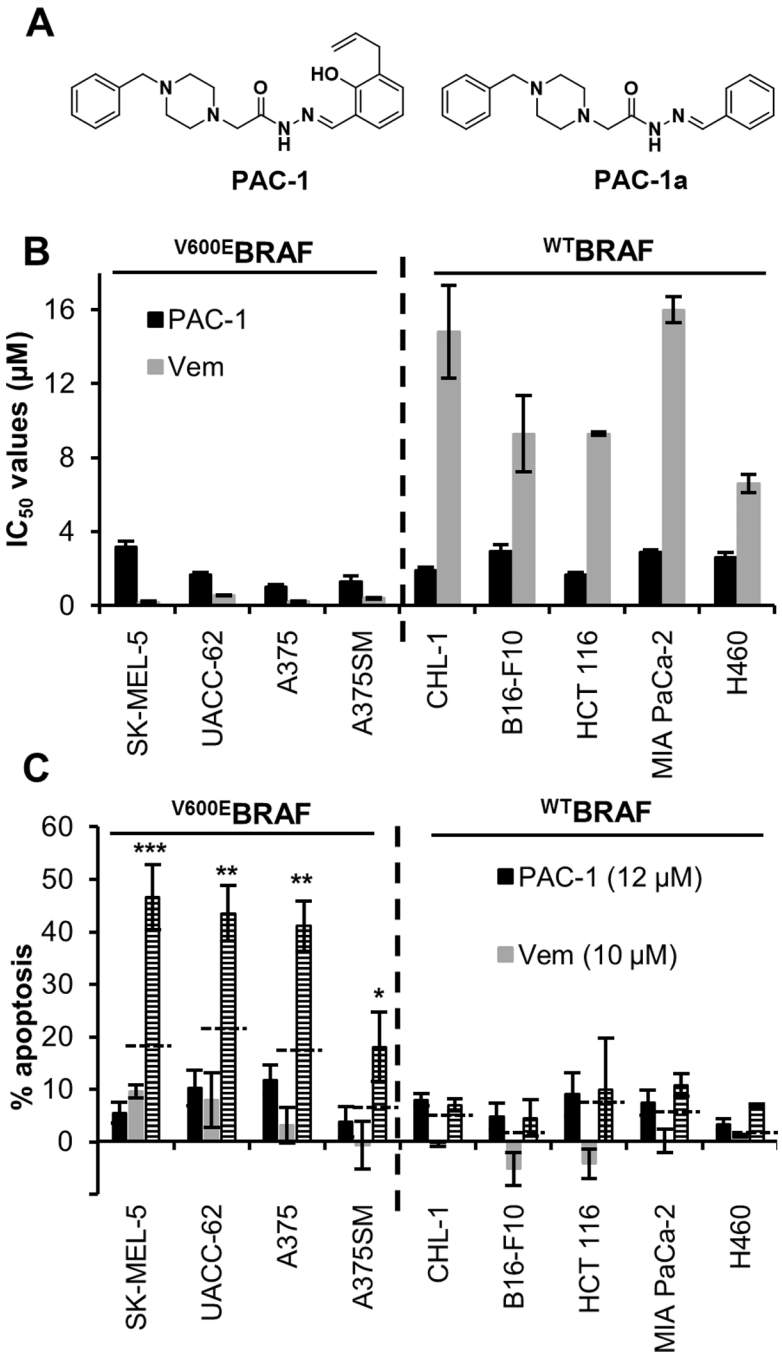

Figure 1.

The effect of vemurafenib and PAC-1 in ^{V600E}BRAF or ^{WT}BRAF cell lines. (**A**) Structure of PAC-1 and PAC-1a. (**B**) IC_{50} values (5 day) of vemurafenib and PAC-1 in a panel of nine cell lines. (**C**) Cell lines with ^{V600E}BRAF have significantly higher percent of cells undergoing apoptosis (assessed by Annexin V-FITC/PI staining) after treatment with vemurafenib (10 μM) and PAC-1 (12 μM) for 24 h, whereas this combination has negligible effect on cell lines with wild-type BRAF. Dashed horizontal lines represent the level of cell death expected from a mere additive effect of the two agents. Values are reported as mean ±

SEM of at least three independent experiments. P-values shown for 2-way interaction to determine if the combination for induction of apoptosis is different from an additive effect (dashed horizontal lines) of individual agents are statistically significant (* $p<0.05$, ** $p<0.01$, *** $p<0.001$).

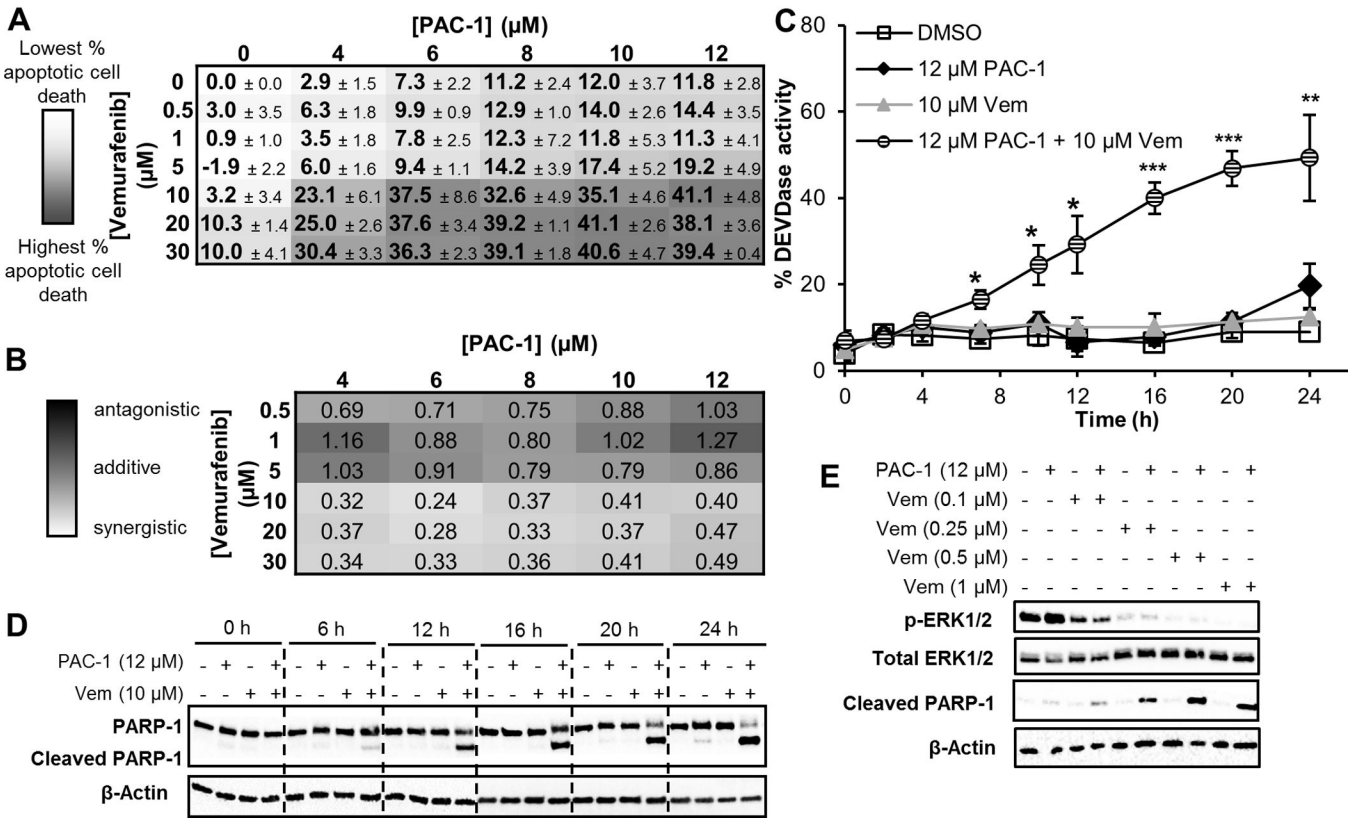

Figure 2.

PAC-1+vemurafenib powerfully synergize to induce apoptotic death and caspase activity in A375 cells. (**A**) Shown is percent apoptotic cell death (assessed by Annexin V/PI staining and flow cytometry) induced after 24 h of treatment. Values shown are heat mapped with white representing low % apoptotic cell death and dark gray representing high % apoptotic cell death. (**B**) Combination indices (CI) calculated for each combination with Combosyn software. CI values are heat mapped with lowest values in light gray and the highest values in black. (**C**) Significant caspase-3/-7 enzymatic activity is observed in cells treated with the combination of PAC-1 and vemurafenib. PAC-1 (12 μM) and vemurafenib (10 μM) alone have little effect (p-values vs. DMSO control > 0.1 at all timepoints). Caspase-3/-7 activity in cell lysates was assessed with the fluorogenic Ac-DEVD-AFC substrate. Activity is expressed as normalized to minimal and maximal activity observed within the assay, with 1 μM staurosporine (STS) as the positive control. (**D**) PAC-1 (12 μM) and vemurafenib (10 μM) alone have little effect on PARP-1 cleavage in A375 cells, but significant PARP-1 cleavage is observed via Western blot with the combination. (**E**) After 24 h, no/low inhibition of ERK1/2 phosphorylation was observed at low concentrations of vemurafenib (0.1 μM and 0.25 μM). At higher concentrations of vemurafenib (0.5 μM and 1 μM), phosphorylation of ERK1/2 was effectively inhibited with or without addition of PAC-1, indicating that effect of PAC-1 is downstream of the MAPK pathway. However, cleaved PARP-1 was only observed in cells treated with the vemurafenib/PAC-1 combination, even at concentrations of vemurafenib (0.1 and 0.25 μM) where incomplete inhibition of ERK1/2 phosphorylation was observed. Values are reported as mean ± SEM of at least three

experiments. P-values shown for 2-way interaction to determine if the combination is different from additive are statistically significant at indicated timepoints. (* $p<0.05$, ** $p<0.01$, *** $p<0.001$)

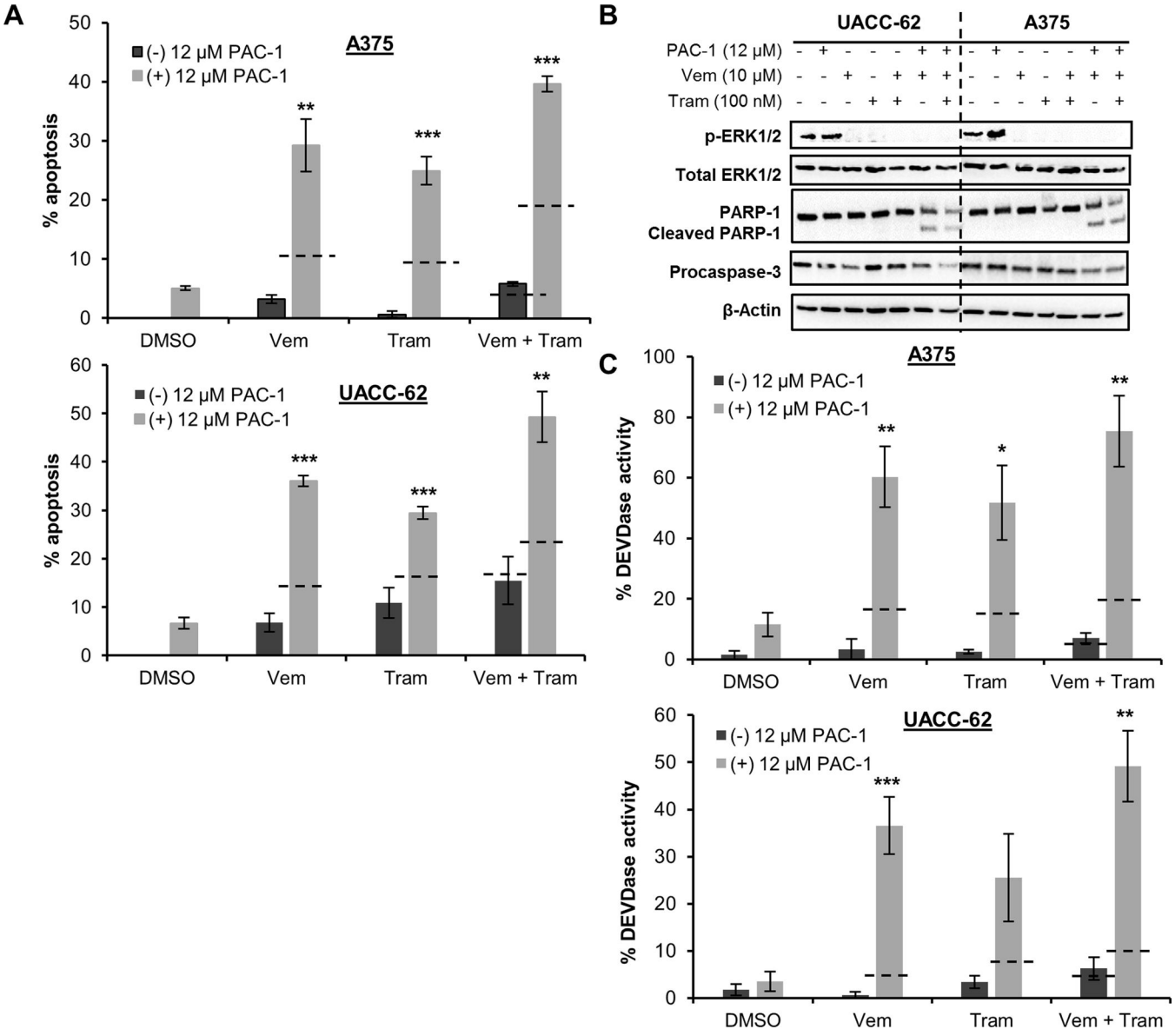

Figure 3.

Addition of PAC-1 to the combination of vemurafenib+trametinib powerfully synergizes to induce apoptotic death and caspase activity in A375 and UACC-62 cells. (**A**) Shown is percent apoptotic cell death after 24 h of treatment. Combination of trametinib (100 nM) and vemurafenib (10 μM) leads to a minimal increase in the population of apoptotic cells. Addition of PAC-1 (12 μM) leads to a dramatic increase in the population of apoptotic cells that is beyond the additive effect of the three agents. (**B**) Trametinib (100 nM) and vemurafenib (10 μM) in combination have little effect on PARP-1 cleavage in A375 and UACC-62 cells, but significant PARP-1 cleavage and reduction in procaspase-3 level are observed via Western blot with the addition of PAC-1 (12 μM). (**C**) Combination of vemurafenib and trametinib lead to additive increase in caspase-3/-7 activity but addition of PAC-1 leads to significant increases in caspase-3/-7 enzymatic activity in A375 and UACC-62 after 24 h. PAC-1 (12 μM), vemurafenib (10 μM) and trametinib (100 nM) alone

have little effect (p-values vs. DMSO control > 0.1). Activity is expressed as normalized to the positive control. Dashed horizontal lines represent the level of cell death expected from a mere additive effect of the two agents. Values are reported as mean ± SEM of at least three experiments. P-values shown for 2-way interaction to determine if the combination for induction of apoptosis is different from an additive effect of individual agents are statistically significant (* $p<0.05$, ** $p<0.01$, *** $p<0.001$).

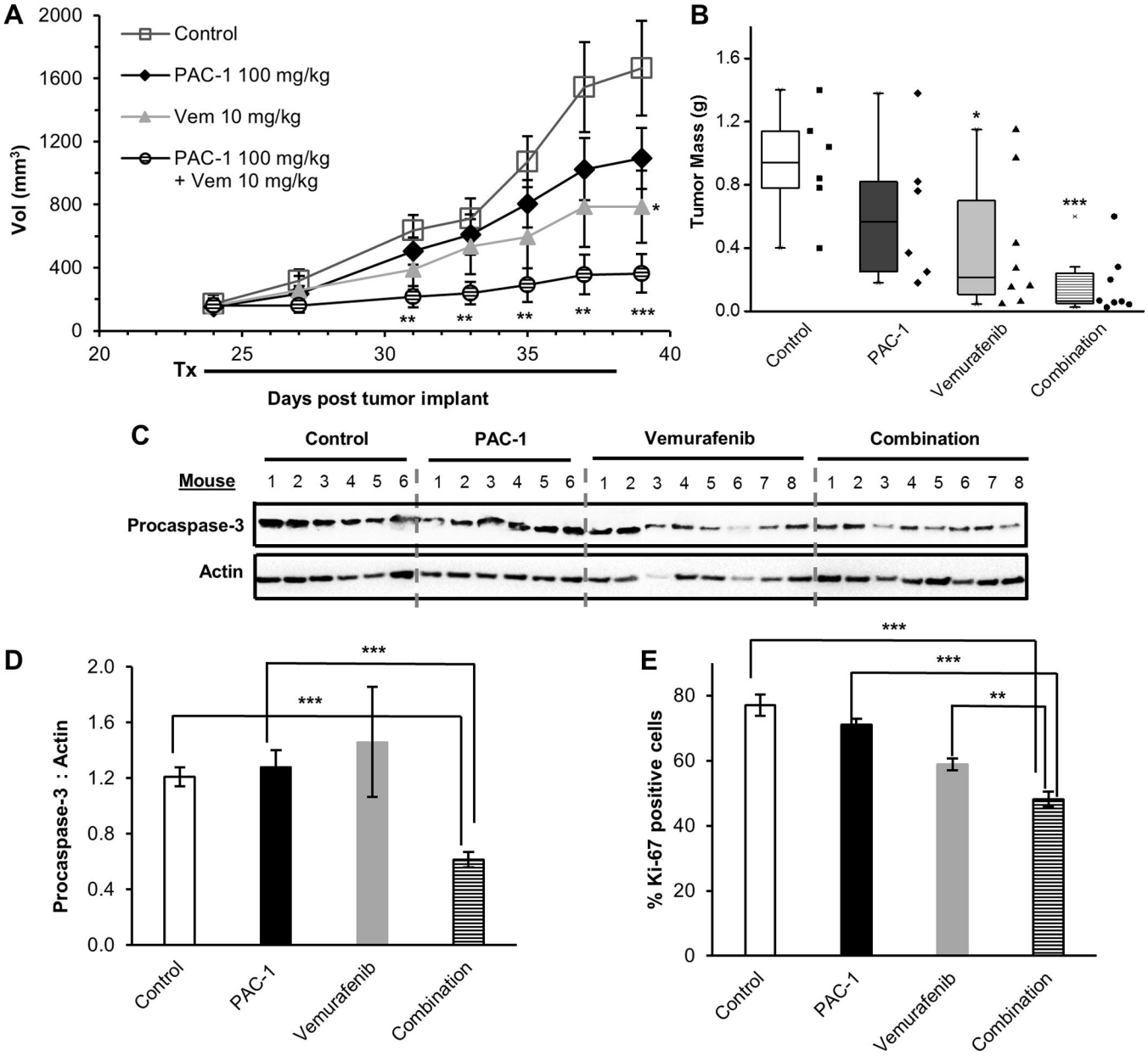

Figure 4.

The PAC-1+vemurafenib combination retards tumor growth in an A375 subcutaneous mouse xenograft model of melanoma. (**A**) The effect of PAC-1, vemurafenib, and their combination in the A375 model. Mice bearing subcutaneous tumors were dosed for 15 days. Mice were dosed with PAC-1 once daily at 100 mg/kg (n=6) via i.p. injection, vemurafenib twice daily at 10 mg/kg (n=8) by (p.o.), or the PAC-1+vemurafenib combination (n=8). The black line below the x-axis indicates the dosing period for the mice during the study. Tumor volumes are plotted as mean ± SEM. (**B**) Masses of the excised tumors. (**C**) Tumor lysates were analyzed by Western blot for changes in procaspase-3 levels. Actin was used as loading control. Band intensity was quantified using ImageJ. (**D**) Plot of procaspase-3 levels normalized to the actin loading controls. (**E**) Percentage of cells that are positive for Ki-67

following immunohistochemical staining of formalin fixed tumor samples. 2000 cells were counted in each sample for each of the four treatment groups. P-values shown are with respect to control mice. (* $p<0.05$, ** $p<0.01$, *** $p<0.001$)

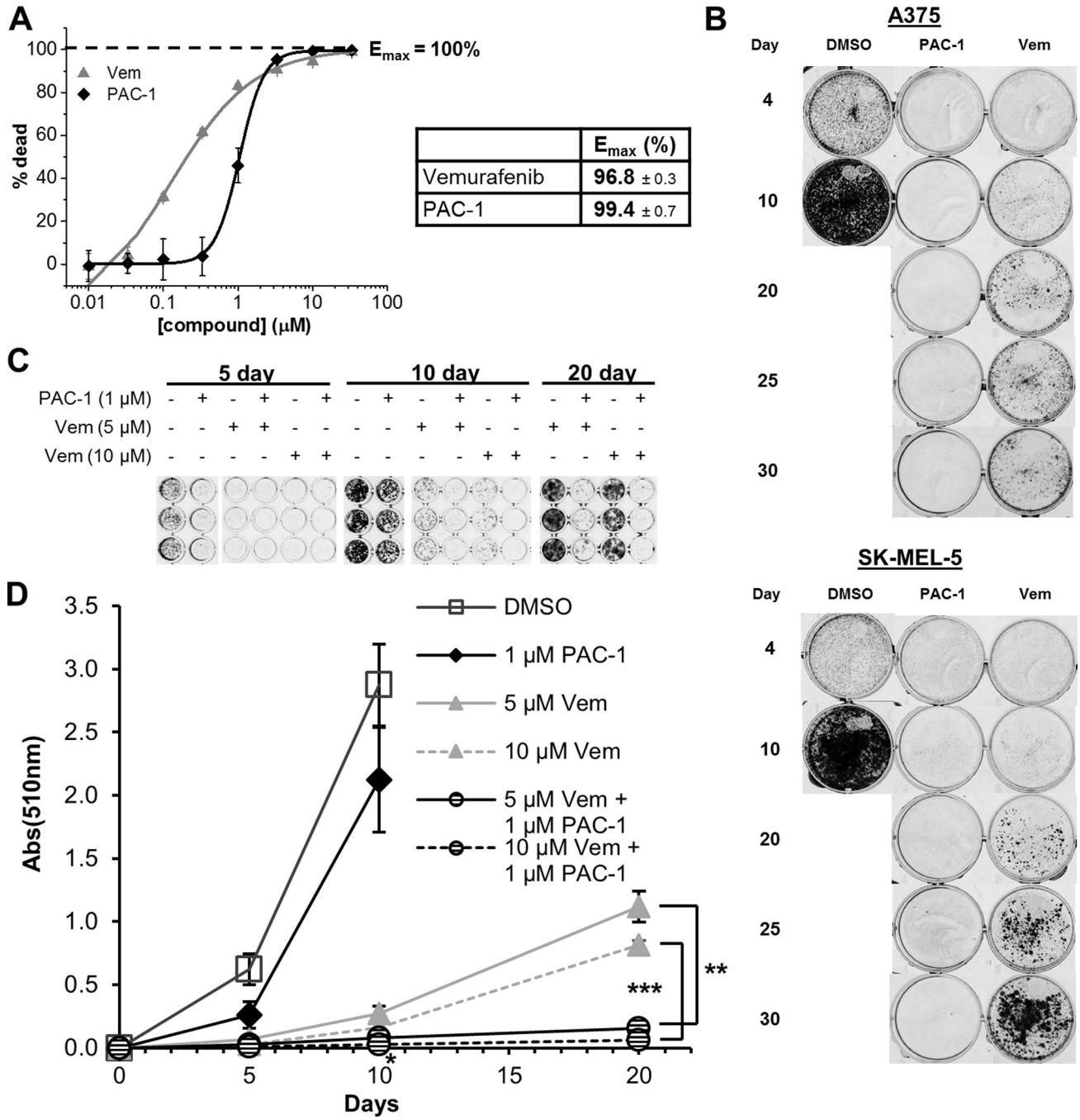

Figure 5.

Low concentrations of PAC-1 (1 μM) significantly delay cell regrowth in combination with vemurafenib in long-term cell culture experiments. (**A**) Comparison of E_{max} values in A375 cells treated with vemurafenib and PAC-1. (**B**) A375 and SK-MEL-5 cells treated with PAC-1 (4 μM) or vemurafenib (10 μM) for a duration of 30 days. (**C**) A375 cells were treated with PAC-1 (1 μM), vemurafenib (5 μM or 10 μM), or the combination. After 5, 10 or 20 days, the wells were fixed with 10% trichloroacetic acid, stained with 0.5% sulforhodamine B (SRB) dye, and imaged with BioRad GelDoc RX. Day 20 images of

control and PAC-1 samples are not shown because the cells were unviable due to overcrowding. (**D**) Quantification of (**C**) where the SRB dye is dissolved in 10 mM Tris base at pH 10.4, and the absorbance read at 510 nm. Corrected absorbance at 510 nm was plotted against the days of continuous treatment by normalizing against absorbance on Day 0 before the start of treatment. Values are reported as mean ± SEM of at least three experiments. T-test performed between wells treated with vemurafenib only versus vemurafenib and PAC-1 (1 μM). On day 10, only the wells treated with vemurafenib (10 μM) and PAC-1 (1 μM) is significantly different from vemurafenib (10 μM) only ($p=0.049$) treatment. On day 20, wells treated with vemurafenib (5 or 10 μM) and PAC-1 (1 μM) are significantly different from vemurafenib (5 or 10 μM), as indicated. (* $p<0.05$, ** $p<0.01$, *** $p<0.001$)

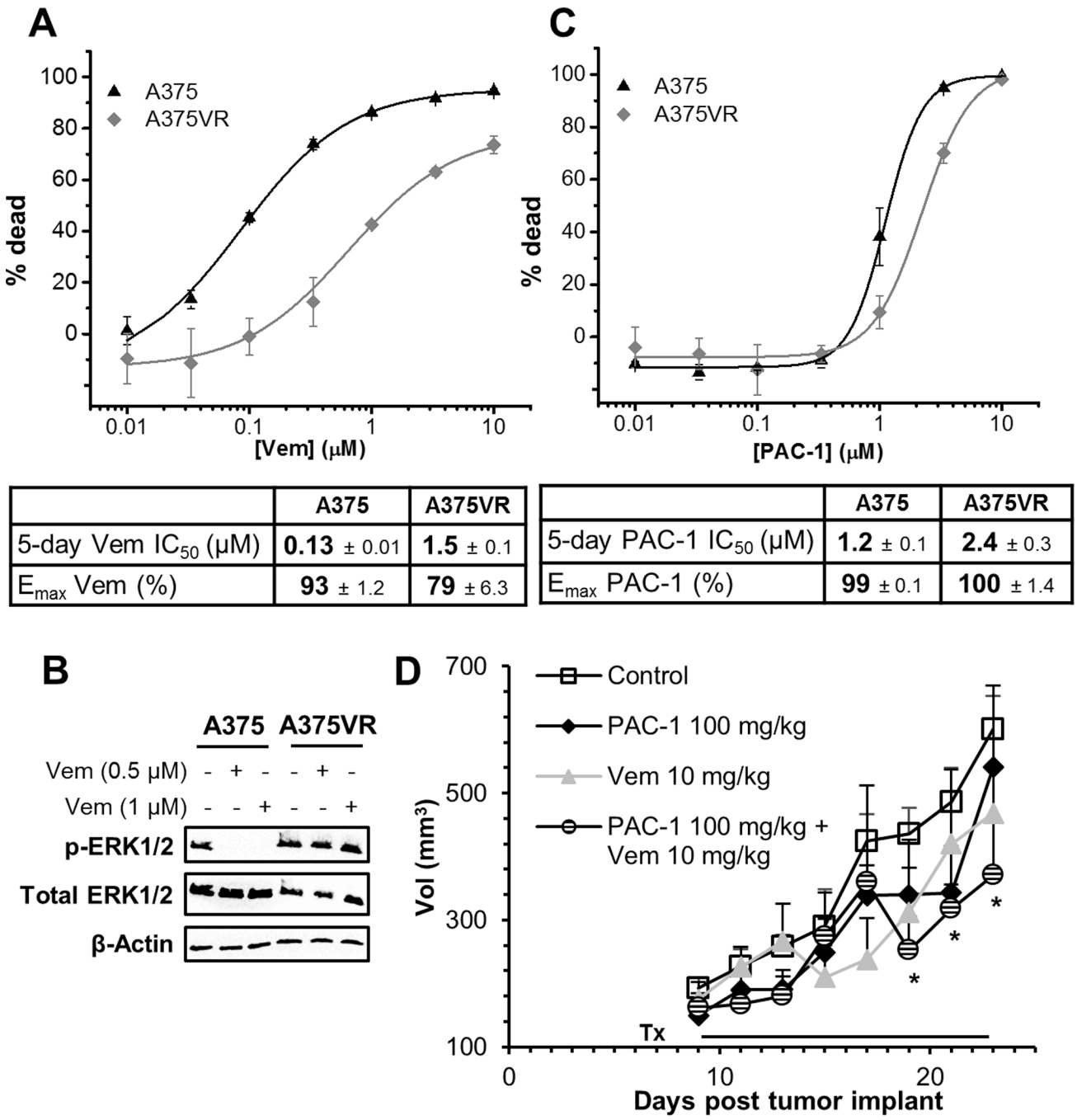

	A375	A375VR
5-day Vem IC_{50} (μM)	**0.13** ± 0.01	**1.5** ± 0.1
E_{max} Vem (%)	**93** ± 1.2	**79** ± 6.3

	A375	A375VR
5-day PAC-1 IC_{50} (μM)	**1.2** ± 0.1	**2.4** ± 0.3
E_{max} PAC-1 (%)	**99** ± 0.1	**100** ± 1.4

Figure 6.

PAC-1 retains activity in vemurafenib-resistant A375VR cells (**A**) Vemurafenib is significantly less active in A375R versus parent A375. (**B**) Treatment with 0.5 or 1 μM of vemurafenib is unable to inhibit phosphorylation of ERK1/2 in A375VR after 2 h. Under the same conditions, complete inhibition of ERK1/2 phosphorylation was observed in the parental A375 cell line. (**C**) PAC-1 retains activity in the A375R cell line. Values are reported as mean ± SEM of at least three independent experiments. (**D**) The effect of PAC-1, vemurafenib, and their combination in the A375VR xenograft model. Mice bearing

subcutaneous tumors were dosed for 15 days. Mice were dosed with PAC-1 twice daily at 100 mg/kg (n=7) by i.p. injection, vemurafenib twice daily at 10 mg/kg (n=5) by (p.o.), or the PAC-1+vemurafenib combination (n=5). The black line above the x-axis indicates the dosing period for the mice during the study. Tumor volumes are plotted as mean + SEM. P-values shown are with respect to control mice. (* $p<0.05$)